Ahmed M. AGWA[1], Mohammed ALRUWAILI[1]

Northern Border University (1)

doi:10.15199/48.2024.11.10

MPPT of PEM Fuel Cell Using DC-DC Boost Converter Based on SVM

Abstract. *Detrimental environmental influences and restricted quantities of conventional energies impose the employment of renewable energies (REs). Regrettably, REs for instance wind and solar energies are sporadic, therefore they have to be stored in different forms for employment throughout their absenteeism. For that purpose, REs can be stored excellently through generation of hydrogen using electrolyzer throughout abundance, then generation of electricity using fuel cell (FC) throughout their absenteeism. Concerning the merits of the proton exchange membrane FC (PEMFC), it is recommended more than different types of FCs. The PEMFC power lacks constancy, as it relies on pressure of hydrogen, temperature, and loading. Hence, a maximum power point tracking (MPPT) technique have to be employed with PEMFC. The procedures formerly employed possess some demerits, for instance delay of reaction, immensity of oscillation, and hugeness of overshoot and undershoot, accordingly this research addresses a PEMFC MPPT based on support vector machine (SVM). Simulation findings of employing the SVM for PEMFC MPPT expose its merits over other techniques in terms of equilibrium among speediness of reaction, tininess of oscillations, and smallness of overshoot and undershoot.*

Streszczenie. *Niekorzystne wpływy środowiskowe i ograniczone ilości konwencjonalnych energii wymuszają wykorzystanie odnawialnych źródeł energii (RE). Niestety, RE, na przykład energia wiatrowa i słoneczna, są sporadyczne, dlatego muszą być przechowywane w różnych formach do wykorzystania w czasie nieobecności. W tym celu RE mogą być doskonale przechowywane poprzez wytwarzanie wodoru za pomocą elektrolizera w obfitości, a następnie wytwarzanie energii elektrycznej za pomocą ogniwa paliwowego (FC) w czasie nieobecności. Jeśli chodzi o zalety membrany wymiany protonów FC (PEMFC), jest ona bardziej zalecana niż inne typy FC. Moc PEMFC nie jest stała, ponieważ opiera się na ciśnieniu wodoru, temperaturze i obciążeniu. Dlatego też w przypadku PEMFC należy zastosować technikę śledzenia maksymalnego punktu mocy (MPPT). Wcześniej stosowane procedury mają pewne wady, na przykład opóźnienie reakcji, ogrom oscylacji i ogrom przekroczenia i niedoregulowania, dlatego też niniejsze badania dotyczą MPPT PEMFC opartego na maszynie wektorów nośnych (SVM). Wyniki symulacji wykorzystującej SVM do pomiaru MPPT PEMFC ujawniają jej zalety w porównaniu z innymi technikami w zakresie równowagi między szybkością reakcji, niewielkimi oscylacjami oraz niewielkimi przekroczeniami i niedoregulowaniami.* (***MPPT ogniwa paliwowego PEM wykorzystującego przetwornik podwyższający napięcie DC-DC oparty na SVM***)

Keywords: MPPT; PEMFC; DC-DC Boost Converter; SVM.
Słowa kluczowe: MPPT; PEMFC; Przetwornica podwyższająca napięcie DC-DC; SVM

Introduction

The transition from traditional energy sources reliant on fossil fuels to renewable energy (RE) is becoming increasingly necessary due to environmental concerns and the ongoing of fossil fuels depletion. RE is eco-friendly and its sources are sustainable. However, their availability can be inconsistent. For instance, wind patterns fluctuate, leading to variable wind speeds that sometimes fall below the minimum required for generating electricity. Similarly, solar energy is unavailable during nighttime and under cloudy conditions. This inherent intermittency of sources like solar and wind power is a notable drawback of REs. As a result, it is essential to store RE to ensure a continuous supply of electrical energy [1,2]. There are various energy storage (ES) methods encompassing chemical, magnetic, mechanical, electrical, electrochemical, thermal, and biological ES. The selection of an ES system largely depends on the type of energy source, the specific energy needs of the application, available funding, and the practicality of the existing system infrastructure [3,4].

Fuel cells (FCs) provide a viable option for converting energy from intermittent renewable sources into usable power, bypassing the need for traditional combustion methods. Surplus RE energy can be stored in the form of hydrogen which is produced using electrolyzers and can be used for electrical energy generation whenever needed using FC.

FCs are categorized in accordance with their electrolyte kind, affecting their function, temperature range, and other features. The proton exchange membrane FC (PEMFC) has several distinguishing advantages compared to other FC technologies, such as the ability to operate at lower temperatures, produce greater power, start-up rapidly, experience little corrosion, utilize a simpler composition, and a smaller volume [5,6]. Given its merits over other FC types, the PEMFC is used in various applications that include distributed generators, transportation, and aviation.

For every specific operational scenario of PEMFC, which includes varying hydrogen pressure P_{H2}, FC temperature T_{fc}, and resistive load (R), there is a distinct point on the current-power (I-P) diagram that represents the maximum power point (MPP). To effectively extract this optimal power from the PEMFC under different conditions, the MPP tracking (MPPT) process is essential. The MPPT system operates using a DC-DC boost converter (DC-DC_BC), which features an adjustable duty switch cycle (DSC).

Various MPPT techniques have been applied to PEMFCs, including incremental resistance [7], incremental conductance [8], perturb and observe (P&O) [9,10], artificial neural network (ANN) [11-14], variable step size (VSS) [15-17], fuzzy logic (FL) [18-20], indirect P&O FL-based VSS [21], and FL controller [22-24].

Beyond the aforementioned techniques, several additional techniques have been implemented for PEMFC MPPT. These include the sliding mode controller [25-27], neuro-fuzzy controller [28-30], model predictive control [31], proportional-integral-derivative (PID) controller, whose gains have been optimized using various algorithms such as the particle swarm optimizer [32], salp swarm approach [33], and grey wolf optimizer [34], and the fractional-order PID controller (FOPID) adjusted via forensic-founded investigation algorithm [35].

In this study, support vector machine (SVM) is innovatively suggested for modelling PEMFC to determine the MPP required for MPPT. SVM is one of the standard machine learning approaches which produces supervised max-margin models through accompanying learning processes that classify and regress data [36]. SVM was employed effectively for MPPT of photovoltaic [37,38]. Additionally, SVM was employed effectively for modelling PEMFC [39-41] but it has not been employed for PEMFC MPPT yet.

The contributions of our study are:

- The innovative utilization of SVM for PEMFC MPPT.
- Comparing the findings of SVM for PEMFC MPPT with the P&O technique, FOPID, and PID controllers to establish its superiority.
- The performance of SVM is legalized via changing P_{H2}, T_{fc}, and R.

The remnant of the study is divided as following: The PEMFC is modelled in Section 2. The DC-DC_BC is described in Section 3. The SVM is clarified in Section 4. The suggested control technique of MPPT is explained in Section 5. The findings are analyzed in Section 6. Deducing the conclusions is in Section 7.

Model of PEMFC

Many illustrations of the PEMFC stack model may be found in the literature. The stack voltage V_{sta} of a quantity of series connected cells (N_c), is determined as follows [15,17]:

(1) $$V_{sta} = N_c \cdot (E - V_{ohm} - V_a - V_{con})$$

where E symbolizes open circuit voltage, V_{ohm} symbolizes ohmic voltage drop for every cell, and V_{con} and V_a symbolize concentration and activation over-voltages for every cell, respectively. Equations (2) to (5) are used to determine the stack voltage parameters.

(2) $$V_a = -[\xi_1 + \xi_2 T_{fc} + \xi_3 T_{fc} \ln(CON_{O_2}) + \xi_4 T_{fc} \ln(I_{fc})]$$

where $\xi_m (m = 1 \text{ to } 4)$ are experimental coefficients, CON_{O2} is O_2 concentration (mol/cm^3), and I_{fc} is the PEMFC working current (A).

(3) $$E = 1.299 - 0.85 \times 10^{-3}(T_{fc} - 298.15) + 4.3085 \times 10^{-5} T_{fc} \ln(P_{H_2} \sqrt{P_{O_2}})$$

where T_{fc} is temperature (K) of cell, and P_{O_2} and P_{H_2} are partial pressures (atm) of O_2 and H_2, respectively.

(4) $$V_{ohm} = I_{fc}(R_{me} + R_{co})$$

where R_{CO} and R_{me} are resistances of the connections and membrane (Ω), respectively.

(5) $$V_{con} = -D \cdot \ln\left(\frac{J_{max} - J}{J_{max}}\right)$$

where D denote parametric factor, and J_{max} and J symbolize maximum and actual denseness of current (A/cm^2), respectively. The stack power P_{sta} can be calculated as:

(6) $$P_{sta} = V_{sta} \cdot I_{fc}$$

(a) I-P cs

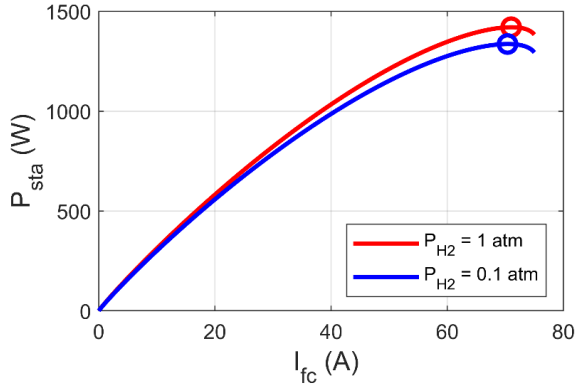

(b) I-V cs

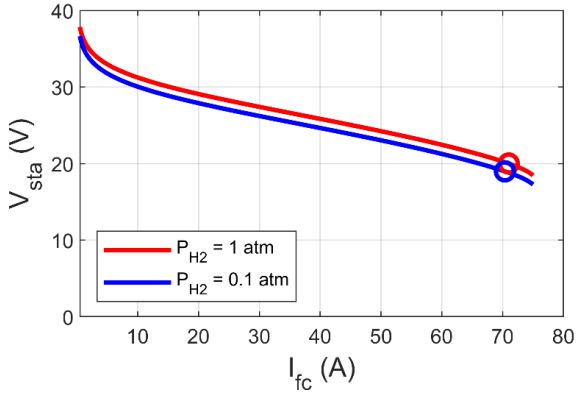

Fig.1. Influence of $P_{(H2)}$ change on MPP of PEMFC.

(a) I-P cs

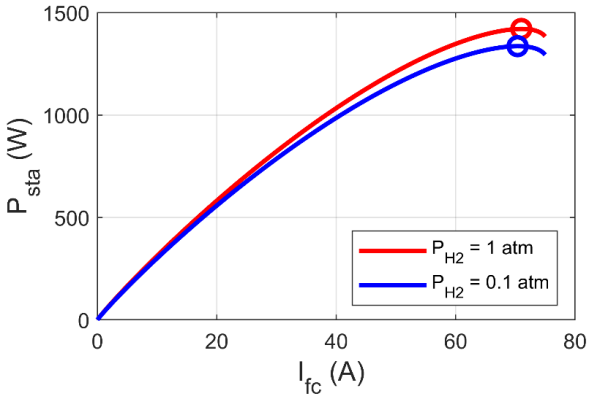

(b) I-V cs

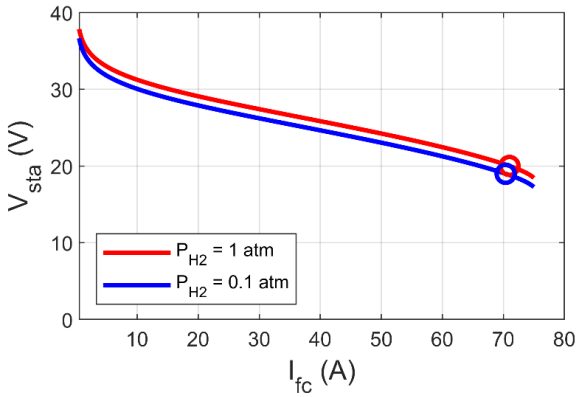

Fig.2 Influence of T_{fc} change on MPP of PEMFC.

The P_{sta} depends on parameters P_{H2}, T_{fc}, and I_{fc} as can be seen in (2)-(5) which are reliant on R. The changes in MPP based on P_{H2} and T_{fc}, respectively, are depicted in Figures 1 and 2, where MPP rises as both P_{H2} and T_{fc} rise. MPP happens at a certain voltage (V_{MP}), which depends on P_{H2}, T_{fc}, and R, as revealed in Figures 1-b and 2-b. Therefore, employing the DC-DC_BC to elevate V_{sta} to V_{MP} is essential for reaching MPP. In this research, we propose a novel PEMFC MPPT that makes use of SVM.

DC-DC Boost Converter

The DC-DC_BC shown in Figure 3 is made up of a capacitor (C) to reduce ripples, a diode (D) to isolate amongst the output and input periods, a MOSFET to turn on and off, and an inductor (L) for storing energy. In addition, the MOSFET gate receives pulses from a pulse width modulator (PWM). Depending on DSC, pulse width is regulated. The switching frequency (f_{swit}) of PWM is used to calculate the amount of pulses per second.

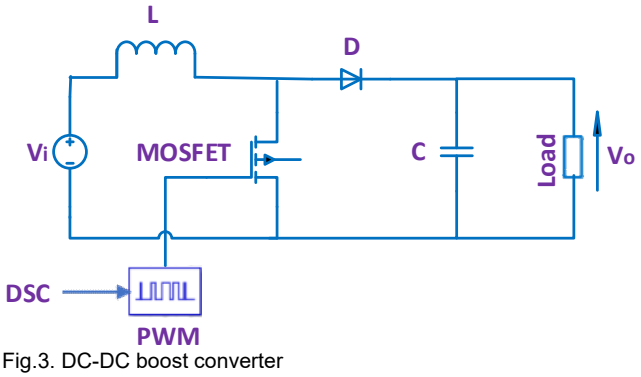

Fig.3. DC-DC boost converter

Equation (7) shows the output voltage (V_o) that is relies on DSC and input voltage (V_i).

(7) $$V_o = \frac{1}{1-DSC} \cdot V_i$$

As shown in (8), DSC can be obtained via (7) for known values of V_i and V_o.

(8) $$DSC = 1 - \frac{V_i}{V_o}$$

In the case of deploying DC-DC_BC for PEMFC MPPT, the DSC needs to be adjusted continually to make V_o tracks V_{MP} continually.

SVM

SVMs are powerful data-driven modelling approaches known for their efficacy in classification and regression problems. SVMs employ a principle called structural risk minimization (SRM), which seeks to minimize a trade-off among the empirical error and the complication of the hypothesis zone. The SVMs regression approaches implying SRM are notable for their robustness and good generalization ability unlike traditional methods like ANN, multiple linear regressions, and partial least squares which are based on reduction of empirical risk [40, 42, 43].

In the SVM regression, only a subset of the training data affects the loss function via an ε-intensive loss function. This approach allows for a balance between minimizing training errors and reducing the complexity of the model. Thus, the greater errors are adjusted using a slack variable since errors littler than ε-intensive loss function are neglected [39]. SVMs are renowned for their effectiveness in high-dimensional spaces and their capability to model complex and nonlinear relationships. They have been effectively utilized in diverse fields, for instance bioinformatics, image processing, and pattern recognition. Several SVM variations have been developed for regression problems, including least squares SVM, v-SVM, and standard SVM (ε-SVM) [40, 43, 44].

The core of SVM lies in constructing an optimum hyperplane in a multidimensional extent to segregate different classes. This is achieved through the following function.

(9) $$G(y) = (u, z) + C$$

where y represents input features, G is the weight vector, and C denotes the bias. The focus of SVMs is to maximize the margin among the hyperplane and the nearest data points of every class, named support vectors [41]. For complex and non-linear datasets, SVM regression is expressed as:

(10) $$(u, z) = \sum_{l=1}^{J^{SVM}} (w_j^+ - w_j^-)\, K(z_j, z)$$

where $K(z_j, z)$ is the kernel function, J^{SVM} is the amount of support vectors, and w_j^+, w_j^- are the model coefficients. For regression tasks, termed support vector regression (SVR), the objective is to fit a function within a defined margin of tolerance, ε. Thus, (10) can be reformulated as:

(11) $$G(y) = \sum_{l=1}^{J^{SVM}} (w_j^+ - w_j^-)\, K(z_j, z) + C$$

According to the SVR principle, (11) can be flatten and subject to the functional minimum that manages the classification margin and error tolerance as shown below:

(12) $$\emptyset(u, \tau) = (0.5) \parallel u \parallel^2 + b \cdot \sum_{l=1}^{J} (\tau_j^- + \tau_j^+)$$

(13) $$L_\varepsilon(x, f(y, \beta)) = |x - f(y, \beta| \varepsilon = \begin{cases} 0, & \text{if } |x - f(y, \beta| \leq \varepsilon \\ \text{else}, & |x - f(y, \beta| - \varepsilon \end{cases}$$

where b represents a predefined constant. The ε-insensitive loss function is employed by the regression process to characterize the deviation between the true and estimated functions, G(y). Larger errors are rejected, but those smaller than ε are accepted [41]. The regression can be transformed to a convex optimization problem as below:

(14) $$\emptyset(u, \tau) = (0.5) \parallel u \parallel^2 + b \cdot \sum_{l=1}^{J} (\tau_j^- + \tau_j^+)$$

(15) $$S.T. \begin{cases} L_\varepsilon(x, f(y, \beta)) \\ \tau_j^- + \tau_j^+ > 0 \end{cases}$$

where τ_j^- and τ_j^+ are slack variables and $\parallel u \parallel^2$ is the norm of u. The minimum of $(0.5) \parallel u \parallel^2$ indicates that G(y) should be flat.

MPPT Control Technique

Figure 4 exposes the proposed control technique for PEMFC MPPT, where DSC of the DC-DC_BC is adjusted utilizing (8) whose inputs are Vo and VMP for making Vo tracks VMP continually, and therefore P_{sta} tracks MPP continually. Vo is fed back from the output of DC-DC_BC while VMP is obtained via SVM model of PEMFC.

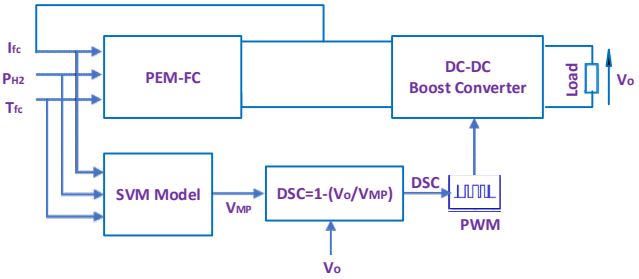

Fig.3. The proposed MPPT control technique.

Results with Discussion

The forcefulness and efficacy of PEMFC MPPT exploiting SVM are evidenced through comparison of its simulation findings with other techniques. The influence of changes in P_{H2}, T_{fc}, and R on the working of the proposed PEMFC MPPT is also investigated.

The SVM is run with these factors: b = 300 and u = 0.045 that were determined based on review of the SVM literature as well as trial and error. The MPPT is run on an industrial classic PEMFC i.e., the Ballard Mark V, whose rated power is 1500 W. In the simulation, 13 measurements of I-V cs are employed for training SVM to model PEMFC at regular P_{H2} and T_{fc} as detailed in Table 1. The measurements change as P_{H2} and/or T_{fc} change. Concerning the value of factors of the DC-DC_BC, f_{swit} = 10

kHz, high value of f_{swit} is decided to lessen the capacitors and inductors, that results in a cost saving, C = 1500 μF, and L = 69 mH. The values of C and L are thoroughly chosen to guarantee low ripples in V_o at the indicated f_{swit}.

Table 1. The measurements of I-V cs employed for SVM model.

I_{fc} (A)	V_{sta} (V)
71.852	19.6
67.298	21
61.226	22.05
56.166	23.8
48.07	24.5
43.01	25.2
37.444	26.25
34.408	26.6
27.83	28
20.24	28.7
16.192	29.75
10.626	30.8
5.06	33.25

PEMFC MPPT at Regular Working Circumstances

Regular working circumstances of P_{H2} and T_{fc} for the investigated PEMFC are utilized in this subsection for various techniques of PEMFC MPPT. In depth, P_{H2}=1 atm and T_{fc} =343 K. Concerning the electric loading, PEMFC is loaded using R of 50 Ω.

Figure 5 exposes P_{sta} of the investigated PEMFC when three MPPT techniques, in addition to the suggested SVM technique, are operated. Particularly, the P&O technique [10], PID and FOPID controllers optimized by golden jackal optimization algorithm (GJOA) [45], are compared with the suggested SVM technique. There is high overshoot in the reaction of P_{sta} during utilization of the P&O technique. Oscillations and slowness exist in the reaction of P_{sta} during utilization of GJOA-FOPID and GJOA-PID controllers. The resulting rise time (t_r) and overshoot in percentage (OSP) for numerous MPPT techniques are recorded in Table 2. The suggested SVM technique results in an OSP of 7.14% which is less than P&O technique but higher than GJOA-FOPID and GJOA-PID controllers. The resultant tr of the suggested SVM technique is 0.25 s, which is lower than GJOA-FOPID and GJOA-PID controllers but higher than P&O technique. The comparison criterion is that the MPPT technique, which possesses the fastest reaction, the lowest oscillations, and the least overshoot, is favoured over other techniques. When applying this criterion to the findings listed in Table 2, the suggested SVM technique has better balance amongst overshoot and speed than other MPPT techniques.

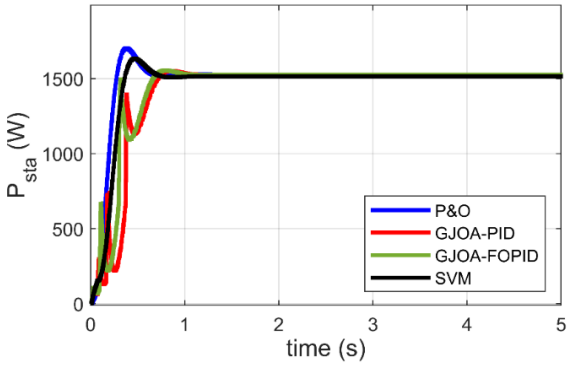

Fig.5. Reaction of PEMFC MPPT techniques.

Table 2. The resultant t_r and OSP for numerous MPPT techniques

MPPT Scheme	t_r (s)	OSP (%)
P&O technique	0.167	11.5
GJOA-FOPID Controller	0.483	1.83
GJOA-PID Controller	0.545	1.46
SVM technique	0.25	7.14

PEMFC MPPT at Varying P_{H2}

In this part, the SVM technique for MPPT of the investigated PEMFC is legalized when P_{H2} varies. Figure 6-a exposes that the P_{H2} has initial value of 1 atm, formerly it rises to 2.3 atm when t=2 s, and then it declines to 1 atm when t=3.5 s. Figure 6-b exposes the reaction of P_{sta} throughout a variation in P_{H2} where MPPT based on SVM is observed to respond hurriedly to changes in P_{H2}. Throughout the stage of rise of P_{H2}, P_{sta} rises to new value afterwards declines with reduction of P_{H2}. This proves that P_{sta} tracks the updated MPP for updated circumstances. The updated circumstances in this case caused by a change of P_{H2} from 1 atm to 2.3 atm and afterwards from 2.3 atm to 1 atm, while T_{fc} and R are constant at 343 K and 50 Ω, respectively. Moreover, the disappearance of oscillations is noticed. Moreover, the overshoot and undershoot are excessively small.

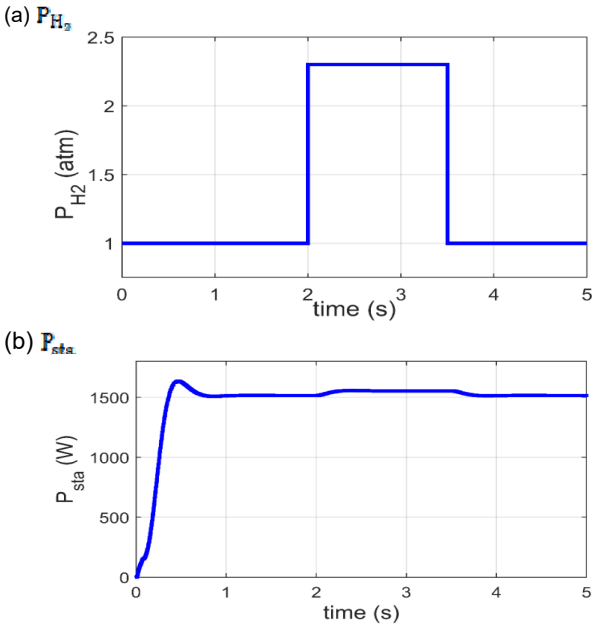

Fig.6. Reaction of PEMFC MPPT based on SVM at varying P_{H_2}.

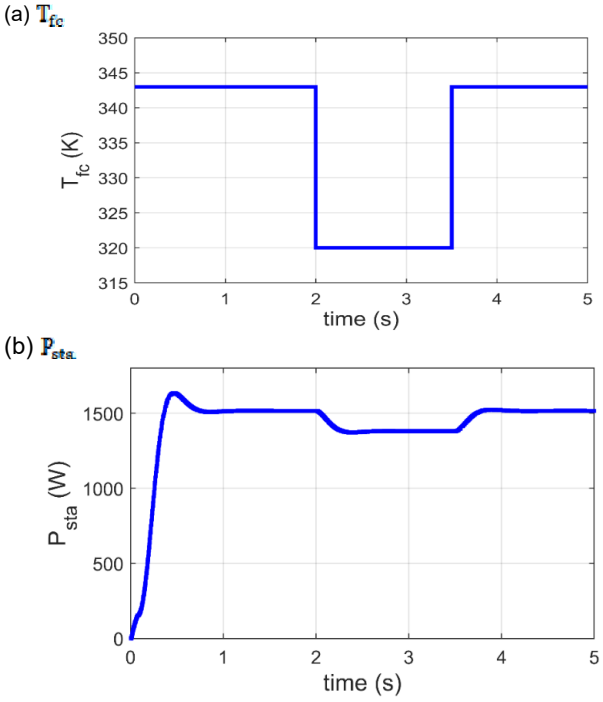

Fig.7. Reaction of PEM-FC MPPT based on SVM at varying T_{FC}.

PEMFC MPPT at Varying T_{fc}

This subsection presents an examination for the SVM for MPPT of the investigated PEMFC when T_{fc} changes. The variation in T_{fc} is presented in Figure 7-a, where the T_{fc} has initial value of 343 K, formerly it declines to 320 K when t=2 s, and then it rises to 343 K when t=3.5 s. The reaction of P_{sta} throughout change of T_{fc} is demonstrated in Figure 6-b, where the rapid working of MPPT exploiting SVM with change of T_{fc} is noticed. During the stage of reduction in T_{fc}, P_{sta} declines to its updated value afterward rises with rise in T_{fc}. This displays that P_{sta} tracks updated MPP for updated circumstances. The updated circumstances in this subsection are resulted by variation in T_{fc} from 343 K to 320 K and afterward from 320 K to 343 K, while P_{H_2} and R are constant at 1 atm and 50 Ω, respectively. Furthermore, there are no oscillations throughout change in P_{sta}.

PEMFC MPPT at Varying R

In this part, SVM for MPPT of the investigated PEMFC is tested when R varies. Figure 8-a shows that R has initial value of 50 Ω, formerly it rises to 54 Ω when t=2 s, and then it declines to 50 Ω when t=3.5 s. Figure 8-b exposes the reaction of P_{sta} throughout variation in P_{H2}, where MPPT exploiting SVM reacts speedily to change in P_{H2}. Throughout the stage of rise in R, P_{sta} declines to its updated value then rises with reduction of R. This certifies that P_{sta} tracks updated MPP for updated circumstances. The updated circumstances in this subsection are resulted by change of R from 50 Ω to 54 Ω and afterward from 54 Ω to 50 Ω, while P_{H2} and T_{fc} are constant at 1 atm and 343 K, respectively. Additionally, the oscillations are small.

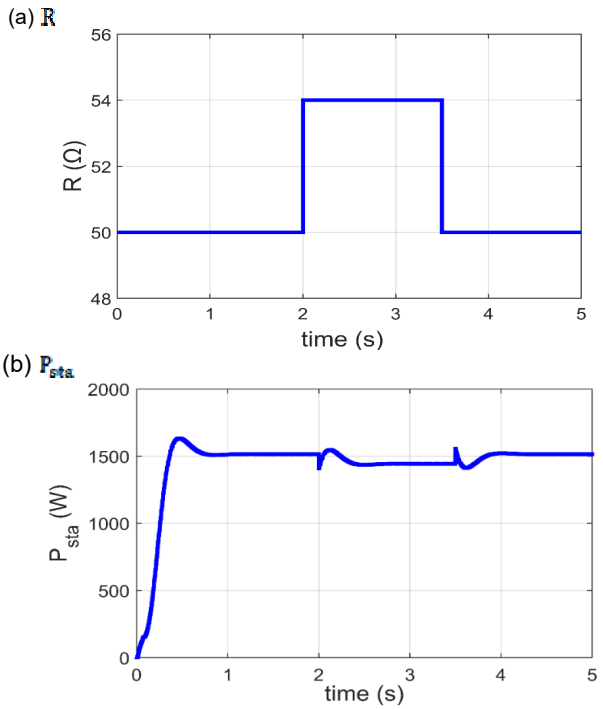

Fig.8. Response of PEMFC MPPT based on SVM at varying R.

Conclusions

The I-P relationship of PEMFC changes according to the working circumstances, viz. P_{H2}, T_{fc}, and R. Therefore, every set of circumstances owns an individual I-P relationship with individual MPP. Consequently, the existence of the MPPT technique is needed to track MPP continually. In this study, an innovative PEMFC MPPT exploiting SVM was suggested. Comparisons of simulation findings were accomplished for the PEMFC MPPT exploiting SVM with other techniques, viz. P&O technique, PID, and FOPID controllers, at regular working circumstances of PEMFC. The comparisons showed that the results using the MPPT technique based on SVM exhibit better balance amongst overshoot and speed compared to other MPPT techniques. Additionally, the PEMFC MPPT exploiting SVM was legitimized throughout change in working circumstances. The simulation findings of the PEMFC MPPT exploiting SVM throughout change of P_{H2}, T_{fc}, and R show the high velocity of performing. Our future research proposal is to empirically validate the proposed PEMFC MPPT technique.

Acknowledgement

The authors gratefully acknowledge the approval and the support of this research study by the grant no. ENGA-2023-12-2355 from the Deanship of Scientific Research at Northern Border University, Arar, K.S.A.

***Authors**: Ahmed M. Agwa, Department of Electrical Engineering, College of Engineering, Northern Border University, Arar 73222, Saudi Arabia, E-mail: ah1582009@yahoo.com.; Mohammed Alruwaili, Department of Electrical Engineering, College of Engineering, Northern Border University, Arar 73222, Saudi Arabia, E-mail: Mohammed.Alruwaili@nbu.edu.sa.*

REFERENCES

[1] A. Dodón, V. Quintero, M. Chen Austin, D. Mora, "Bio-Inspired Electricity Storage Alternatives to Support Massive Demand-Side Energy Generation: A Review of Applications at Building Scale," *Biomimetics*, vol. 6, no. 3, p. 51, Aug. 2021, DOI: 10.3390/biomimetics6030051.

[2] M. Nasser, H. Hassan, "Assessment of standalone streetlighting energy storage systems based on hydrogen of hybrid PV/electrolyzer/fuel cell/ desalination and PV/batteries," *J Energy Storage*, vol. 63, p. 106985, Jul. 2023, DOI: 10.1016/j.est.2023.106985.

[3] M. Calati, K. Hooman, S. Mancin, "Thermal storage based on phase change materials (PCMs) for refrigerated transport and distribution applications along the cold chain: A review," *International Journal of Thermofluids*, vol. 16, p. 100224, Nov. 2022, DOI: 10.1016/j.ijft.2022.100224.

[4] M. Korpås, "Distributed Energy Systems with Wind Power and Energy Storage," Norwegian University of Science and Technology, Trondheim, Norway, 2004.

[5] S. Mekhilef, R. Saidur, A. Safari, "Comparative study of different fuel cell technologies," *Renewable and Sustainable Energy Reviews*, vol. 16, no. 1, pp. 981–989, Jan. 2012, DOI: 10.1016/j.rser.2011.09.020.

[6] Z. Jakšić, O. Jakšić, "Biomimetic Nanomembranes: An Overview," *Biomimetics*, vol. 5, no. 2, p. 24, May 2020, DOI: 10.3390/biomimetics5020024.

[7] H. Rezk, "Performance of incremental resistance MPPT based proton exchange membrane fuel cell power system," in 2016 Eighteenth International Middle East Power Systems Conference (MEPCON), IEEE, Dec. 2016, pp. 199–205. DOI: 10.1109/MEPCON.2016.7836891.

[8] N. Karami, L. El Khoury, G. Khoury, N. Moubayed, "Comparative study between P&O and incremental conductance for fuel cell MPPT," in International Conference on Renewable Energies for Developing Countries 2014, IEEE, Nov. 2014, pp. 17–22. DOI: 10.1109/REDEC.2014.7038524.

[9] V. Karthikeyan, P. V. Das, F. Blaabjerg, "Implementation of MPPT Control in Fuel Cell Fed High Step-up Ratio DC-DC Converter," in 2018 2nd IEEE International Conference on Power Electronics, Intelligent Control and Energy Systems (ICPEICES), IEEE, Oct. 2018, pp. 689–693. DOI: 10.1109/ICPEICES.2018.8897443.

[10] N. Naseri, S. El Hani, A. Aghmadi, K. El Harouri, M. S. Heyine, H. Mediouni, "Proton Exchange Membrane Fuel Cell Modelling and Power Control by P&O Algorithm," in 2018 6th International Renewable and Sustainable Energy Conference (IRSEC), IEEE, Dec. 2018, pp. 1–5. DOI: 10.1109/IRSEC.2018.8703002.

[11] K. J. Reddy, N. Sudhakar, "High Voltage Gain Interleaved Boost Converter with Neural Network Based MPPT Controller for Fuel Cell Based Electric Vehicle Applications," *IEEE*

Access, vol. 6, pp. 3899–3908, 2018, DOI: 10.1109/ACCESS.2017.2785832.
[12] M. Derbeli, C. Napole, O. Barambones, "Machine Learning Approach for Modeling and Control of a Commercial Heliocentris FC50 PEM Fuel Cell System," *Mathematics*, vol. 9, no. 17, p. 2068, Aug. 2021, DOI: 10.3390/math9172068.
[13] K. J. Reddy, N. Sudhakar, "A new RBFN based MPPT controller for grid-connected PEMFC system with high step-up three-phase IBC," *Int J Hydrogen Energy*, vol. 43, no. 37, pp. 17835–17848, Sep. 2018, DOI: 10.1016/j.ijhydene.2018.07.177.
[14] A. Harrag, H. Bahri, "Novel neural network IC-based variable step size fuel cell MPPT controller," *Int J Hydrogen Energy*, vol. 42, no. 5, pp. 3549–3563, Feb. 2017, DOI: 10.1016/j.ijhydene.2016.12.079.
[15] A. Harrag, H. Bahri, "A Novel Single Sensor Variable Step Size Maximum Power Point Tracking for Proton Exchange Membrane Fuel Cell Power System," *Fuel Cells*, vol. 19, no. 2, pp. 177–189, Apr. 2019, DOI: 10.1002/fuce.201800122.
[16] H. Rezk, A. Fathy, "Performance Improvement of PEM Fuel Cell Using Variable Step-Size Incremental Resistance MPPT Technique," *Sustainability*, vol. 12, no. 14, p. 5601, Jul. 2020, DOI: 10.3390/su12145601.
[17] A. Harrag, S. Messalti, "Variable Step Size IC MPPT Controller for PEMFC Power System Improving Static and Dynamic Performances," *Fuel Cells*, vol. 17, no. 6, pp. 816–824, Dec. 2017, DOI: 10.1002/fuce.201700047.
[18] D. N. Luta, A. K. Raji, "Comparing fuzzy rule-based MPPT techniques for fuel cell stack applications," *Energy Procedia*, vol. 156, pp. 177–182, Jan. 2019, DOI: 10.1016/j.egypro.2018.11.124.
[19] M. Gheisarnejad, J. Boudjadar, M.-H. Khooban, "A New Adaptive Type-II Fuzzy-Based Deep Reinforcement Learning Control: Fuel Cell Air-Feed Sensors Control," *IEEE Sens J*, vol. 19, no. 20, pp. 9081–9089, Oct. 2019, DOI: 10.1109/JSEN.2019.2924726.
[20] M. Aliasghary, "Control of PEM Fuel Cell Systems Using Interval Type-2 Fuzzy PID Approach," *Fuel Cells*, vol. 18, no. 4, pp. 449–456, Aug. 2018, DOI: 10.1002/fuce.201700157.
[21] A. Harrag, H. Rezk, "Indirect P&O type-2 fuzzy-based adaptive step MPPT for proton exchange membrane fuel cell," *Neural Comput Appl*, vol. 33, no. 15, pp. 9649–9662, Aug. 2021, DOI: 10.1007/s00521-021-05729-w.
[22] M. J. Khan, L. Mathew, "Fuzzy logic controller-based MPPT for hybrid photo-voltaic/wind/fuel cell power system," *Neural Comput Appl*, vol. 31, no. 10, pp. 6331–6344, Oct. 2019, DOI: 10.1007/s00521-018-3456-7.
[23] F. Aggad, "Modeling, Design and Energy Management of a Residential Standalone Photovoltaic-Fuel Cell Power System," *Przegląd Elektrotechniczny*, vol. 1, no. 8, pp. 81–89, Jul. 2020, DOI: 10.15199/48.2020.08.17.
[24] M. Derbeli, L. Sbita, M. Farhat, O. Barambones, "Proton exchange membrane fuel cell — A smart drive algorithm," in 2017 International Conference on Green Energy Conversion Systems (GECS), IEEE, Mar. 2017, pp. 1–5. DOI: 10.1109/GECS.2017.8066167.
[25] M. H. Wang, M. Huang, W. Jiang, K. Liou, "Maximum power point tracking control method for proton exchange membrane fuel cell," *IET Renewable Power Generation*, vol. 10, no. 7, pp. 908–915, Aug. 2016, DOI: 10.1049/iet-rpg.2015.0205.
[26] M. Derbeli, O. Barambones, M. Farhat, J. A. Ramos-Hernanz, L. Sbita, "Robust high order sliding mode control for performance improvement of PEM fuel cell power systems," *Int J Hydrogen Energy*, vol. 45, no. 53, pp. 29222–29234, Oct. 2020, DOI: 10.1016/j.ijhydene.2020.07.172.
[27] M. Y. Silaa, M. Derbeli, O. Barambones, A. Cheknane, "Design and Implementation of High Order Sliding Mode Control for PEMFC Power System," *Energies*, vol. 13, no. 17, p. 4317, Aug. 2020, DOI: 10.3390/en13174317.
[28] K. J. Reddy, N. Sudhakar, "ANFIS-MPPT control algorithm for a PEMFC system used in electric vehicle applications," *Int J Hydrogen Energy*, vol. 44, no. 29, pp. 15355–15369, Jun. 2019, DOI: 10.1016/j.ijhydene.2019.04.054.
[29] H. Ashraf, M. M. Elkholy, S. O. Abdellatif, A. A. El Fergany, "Synergy of neuro-fuzzy controller and tuna swarm algorithm for maximizing the overall efficiency of PEM fuel cells stack including dynamic performance," *Energy Conversion and Management: X*, vol. 16, p. 100301, Dec. 2022, DOI: 10.1016/j.ecmx.2022.100301.
[30] A. Raj, P. Lekhaj, "An ANFIS Based MPPT Controller for Fuel Cell Powered Induction Motor Drive," in 2018 International Conference on Smart Grid and Clean Energy Technologies (ICSGCE), IEEE, May 2018, pp. 201–205. DOI: 10.1109/ICSGCE.2018.8556712.
[31] M. Derbeli, A. Charaabi, O. Barambones, C. Napole, "High-Performance Tracking for Proton Exchange Membrane Fuel Cell System PEMFC Using Model Predictive Control," *Mathematics*, vol. 9, no. 11, p. 1158, May 2021, DOI: 10.3390/math9111158.
[32] S. Ahmadi, Sh. Abdi, M. Kakavand, "Maximum power point tracking of a proton exchange membrane fuel cell system using PSO-PID controller," *Int J Hydrogen Energy*, vol. 42, no. 32, pp. 20430–20443, Aug. 2017, DOI: 10.1016/j.ijhydene.2017.06.208.
[33] A. Fathy, M. A. Abdelkareem, A. G. Olabi, H. Rezk, "A novel strategy based on salp swarm algorithm for extracting the maximum power of proton exchange membrane fuel cell," *Int J Hydrogen Energy*, vol. 46, no. 8, pp. 6087–6099, Jan. 2021, DOI: 10.1016/j.ijhydene.2020.02.165.
[34] K. P. S. Rana, V. Kumar, N. Sehgal, S. George, "A Novel dP/dI feedback based control scheme using GWO tuned PID controller for efficient MPPT of PEM fuel cell," *ISA Trans*, vol. 93, pp. 312–324, Oct. 2019, DOI: 10.1016/j.isatra.2019.02.038.
[35] A. Fathy, H. Rezk, T. M. Alanazi, "Recent Approach of Forensic-Based Investigation Algorithm for Optimizing Fractional Order PID-Based MPPT With Proton Exchange Membrane Fuel Cell," *IEEE Access*, vol. 9, pp. 18974-18992, 2021, DOI: 10.1109/ACCESS.2021.3054552.
[36] S. Suthaharan, Support Vector Machine. In: Machine Learning Models and Algorithms for Big Data Classification. Integrated Series in Information Systems, vol. 36. Springer, Boston, MA, 2016. DOI: 10.1007/978-1-4899-7641-3_9
[37] P. V. Mahesh, S. Meyyappan, R. Alla, "Support Vector Regression Machine Learning based Maximum Power Point Tracking for Solar Photovoltaic systems," *Int J Elec Comp Eng Sys*, vol. 14, no. 1, pp. 100-108, 2023. DOI: 10.32985/ijeces.14.1.11.
[38] C. González-Castaño, J. Marulanda, C. Restrepo, S. Kouro, A. Alzate, J. Rodriguez, "Hardware-in-the-Loop to Test an MPPT Technique of Solar Photovoltaic System: A Support Vector Machine Approach," *Sustainability*, vol. 13, no. 6, 3000, 2021. DOI: 10.3390/su13063000
[39] A. Kheirandish, N. Shafiabady, M. Dahari, M. S. Kazemi, D. Isa, "Modeling of commercial proton exchange membrane fuel cell using support vector machine," *Int J Hydrogen Energy*, vol. 41, no. 26, pp. 11351–11358, Jul. 2016, DOI: 10.1016/j.ijhydene.2016.04.043.
[40] I. S. Han, C. B. Chung, "Performance prediction and analysis of a PEM fuel cell operating on pure oxygen using data-driven models: A comparison of artificial neural network and support vector machine," *Int J Hydrogen Energy*, vol. 41, no. 24, pp. 10202–10211, Jun. 2016, DOI: 10.1016/j.ijhydene.2016.04.247.
[41] Z. D. Zhong, X.-J. Zhu, G. Y. Cao, "Modeling a PEMFC by a support vector machine," *J Power Sources*, vol. 160, no. 1, pp. 293–298, Sep. 2006, DOI: 10.1016/j.jpowsour.2006.01.040.
[42] I. Han, C. Han, C. Chung, "Melt index modeling with support vector machines, partial least squares, and artificial neural networks," *J Appl Polym Sci*, vol. 95, no. 4, pp. 967–974, Feb. 2005, DOI: 10.1002/app.20979.
[43] B. Zhao, "Modeling pressure drop coefficient for cyclone separators: A support vector machine approach," *Chem Eng Sci*, vol. 64, no. 19, pp. 4131–4136, Oct. 2009, DOI: 10.1016/j.ces.2009.06.017.
[44] C. F. Kung, P. Y. Hao, "Fuzzy Least Squares Support Vector Machine with Fuzzy Hyperplane," *Neural Process Lett*, vol. 55, no. 6, pp. 7415–7446, Dec. 2023, DOI: 10.1007/s11063-023-11267-4.
[45] A. M. Agwa, T.I. Alanazi, H. Kraiem, E. Touti, A. Alanazi, D. K. Alanazi, "MPPT of PEM Fuel Cell Using PI-PD Controller Based on Golden Jackal Optimization Algorithm," *Biomimetics*, vol. 8, no. 5, 4262023, 2023. DOI: 10.3390/biomimetics8050426.